R_{in} (Fig. 4A). The lines were displaced vertically from one another because the different test stimuli and adaptation states shifted the DC membrane potential. There was, however, little effect of visual stimulation (*22*, *23*) or adaptation on the slopes of the current-voltage relation, indicating that R_{in} changed little. This was true on average for all six cells tested; the linear fit through the points of Fig. 4B has a slope of unity and an intercept of <1 megohm, indicating no change in input resistance in the adapted state.

These measurements of R_{in} are more consistent with adaptation being caused by a decrease in tonic excitation than by an increase in tonic inhibition. Supporting evidence for a decrease in excitation underlying adaptation comes from in vitro experiments showing that intracortical synaptic excitation is depressed after repetitive electrical stimulation (*24*). Moreover, antagonists to presynaptic glutamate autoreceptors that mediate excitatory synaptic depression reduce extracellularly measured adaptation effects (*17*). GABA (γ-aminobutyric acid) antagonists, on the other hand, have little effect on adaptation (*17*, *18*). Taken together, these and our observations give strong support for the view that adaptation is caused by a decrease in the excitation received by a cell. In principle, this decrease could originate from an activity-dependent decrease in synaptic efficacy (*24*) whose effect would be enhanced if there were excitatory feedback among cortical cells (*25*). Our results provide the further constraint that adaptation must act largely through a tonic mechanism, which is an indicator of recent contrast history and operates both in the presence and in the absence of visual stimulation.

REFERENCES AND NOTES

1. L. Maffei, A. Fiorentini, S. Bisti, *Science* **182**, 1036 (1973); D. G. Albrecht, S. B. Farrar, D. B. Hamilton, *J. Physiol. (London)* **347**, 713 (1984).
2. R. G. Vautin and M. A. Berkeley, *J. Neurophysiol.* **40**, 1051 (1977).
3. J. A. Movshon and P. Lennie, *Nature* **278**, 850 (1979).
4. I. Ohzawa, G. Sclar, R. D. Freeman, *ibid.* **298**, 266 (1982); *J. Neurophysiol.* **54**, 651 (1985).
5. This phenomenon is uniquely cortical because it is essentially absent at earlier stages of visual processing (*4*) [T. Shou, X. Li, Y. Zhou, B. Hu, *Visual Neurosci.* **13**, 605 (1996)], and stimulation of one eye reduces the responses of cortical cells to stimulation of the other eye [L. Maffei, N. Berardi, S. Bisti, *J. Neurophysiol.* **55**, 966 (1986)].
6. H. B. Barlow, in *Vision: Coding and Efficiency*, C. Blakemore, Ed. (Cambridge Univ. Press, Cambridge, 1990); M. Carandini, H. B. Barlow, L. P. O'Keefe, A. B. Poirson, J. A. Movshon, *Philos. Trans. R. Soc. London Ser. B*, in press.
7. Whole-cell patch recordings in current clamp mode were obtained from barbiturate-anesthetized, paralyzed adult cats (*23*). Drifting sinusoidal gratings (mean luminance 15 cd/m^2) of optimal orientation, direction, spatial and temporal frequency, and window size were presented monocularly on an oscilloscope screen with an image generator (Innisfree, Cambridge, MA).
8. J. A. Movshon, I. D. Thompson, D. J. Tolhurst, *J. Physiol. (London)* **283**, 53 (1978).
9. D. G. Albrecht and D. B. Hamilton, *J. Neurophysiol.* **48**, 217 (1982).
10. This increase in the mean membrane potential with increasing contrast represents a nonlinearity in the responses of simple cells. We propose that it is caused by a differential contrast sensitivity of the excitatory and inhibitory inputs known to underlie the responses of simple cells (*12*). In this scenario, the responses at low contrasts are dominated by excitation, and inhibition appears only at higher contrasts. At low contrasts, increases in contrast cause increases in excitation that are relatively unopposed by increases in inhibition; as a result, the mean membrane potential increases with contrast. At higher contrasts, the inhibitory inputs begin to respond strongly, opposing the effects of increasing excitation and causing the mean potential to stop growing with contrast or even to decrease slightly.
11. C. Blakemore and F. W. Campbell, *J. Physiol. (London)* **203**, 237 (1969).
12. The depolarized portions of the visually driven membrane potential responses of a simple cell are attributable to increases in excitation as well as decreases in inhibition. Similarly, the hyperpolarized portions of these responses are attributable to decreases in excitation as well as increases in inhibition [D. Ferster, *J. Neurosci.* **8**, 1172 (1988)].
13. A. B. Bonds, *Visual Neurosci.* **6**, 239 (1991).
14. J. J. Kulikowski, V. M. Rao, T. R. Vidyasagar, *J. Physiol. (London)* **318**, 21P (1981); A. B. Saul and M. S. Cynader, *Visual Neurosci.* **2**, 593 (1989); S. Marlin, R. Douglas, M. Cynader, *J. Neurophysiol.* **69**, 2209 (1993).
15. J. A. Movshon, I. D. Thompson, D. J. Tolhurst, *J. Physiol. (London)* **283**, 79 (1978).
16. Other possible mechanisms include a long-lasting after-hyperpolarization [P. C. Schwindt *et al.*, *J. Neurophysiol.* **59**, 424 (1988)], an electrogenic pump, and a neuromodulatory effect on voltage-gated channels. Because adaptation could also be observed in the absence of spikes in the recorded cell, we doubt that the first mechanism is at work. It is doubtful that the second mechanism could produce hyperpolarizations as large as 15 mV. Our results, however, would be consistent with the third mechanism.
17. J. McLean and L. A. Palmer, *Visual Neurosci.* **13**, 1069 (1996).
18. E. J. DeBruyn and A. B. Bonds, *Brain Res.* **383**, 339 (1986); T. R. Vidyasagar, *Neuroscience* **36**, 175 (1990).
19. A. B. Saul, *Visual Neurosci.* **12**, 191 (1995).
20. R. S. Dealy and D. J. Tolhurst, *J. Physiol. (London)* **241**, 261 (1974); D. J. Heeger, *Visual Neurosci.* **9**, 181 (1992).
21. Assuming a passive neuron with a single compartment, the change in input resistance needed to hyperpolarize the membrane from V to V_A is $\Delta R_{in} = R_{in}(V_A - V)/(V - E_A)$, where E_A is the reversal potential of the synaptic input responsible for the hyperpolarization, and is 0 mV for excitatory postsynaptic potentials and −90 mV for inhibitory postsynaptic potentials. To produce a hyperpolarization from −65 to −70 mV, a decrease in excitation would require an 8% increase in R_{in}; an increase in inhibition would require a decrease of 20%. Simultaneous changes in excitation and inhibition could, of course, offset one another and result in a zero net change in R_{in}.
22. R. J. Douglas, K. A. C. Martin, D. Whitteridge, *Nature* **332**, 642 (1988).
23. D. Ferster and B. Jagadeesh, *J. Neurosci.* **12**, 1262 (1992).
24. S. B. Nelson, J. A. Varela, K. Sen, L. F. Abbott, in *The Neurobiology of Computation*, J. Bower, Ed. (Kluwer Academic, Boston, in press); E. V. Todorov, A. G. Siapas, D. C. Somers, S. B. Nelson, *ibid.*
25. R. J. Douglas, C. Koch, M. Mahowald, K. A. C. Martin, H. H. Suarez, *Science* **269**, 981 (1995).

26. We thank S. Chung for her contribution to the experiments and N. Spruston for his comments on the manuscript. Supported by National Eye Institute grant EY04726.

3 January 1997; accepted 18 March 1997

Regulation of Protein Phosphatase 2A by Direct Interaction with Casein Kinase 2α

Jean-Karim Hériché, Franck Lebrin, Thierry Rabilloud, Didier Leroy,* Edmond M. Chambaz, Yves Goldberg†

Timely deactivation of kinase cascades is crucial to the normal control of cell signaling and is partly accomplished by protein phosphatase 2A (PP2A). The catalytic (α) subunit of the serine-threonine kinase casein kinase 2 (CK2) bound to PP2A in vitro and in mitogen-starved cells; binding required the integrity of a sequence motif common to CK2α and SV40 small t antigen. Overexpression of CK2α resulted in deactivation of mitogen-activated protein kinase kinase (MEK) and suppression of cell growth. Moreover, CK2α inhibited the transforming activity of oncogenic Ras, but not that of constitutively activated MEK. Thus, CK2α may regulate the deactivation of the mitogen-activated protein kinase pathway.

Down-regulation of the mitogen-activated protein kinase (MAPK) cascade is crucial to normal growth control. PP2A plays an important role in this process by dephosphorylating the activating site in MAPK as well as in the enzyme that activates MAPK, MEK (MAPK or extracellular signal–regulated kinase kinase) (*1*). The core PP2A enzyme is a dimer of one catalytic (PP2Ac) and one regulatory (PR65/A) subunit; an additional, variable regulatory (B) subunit binds to PR65 and confers substrate specificity to the dephosphorylating activity (*2*). The SV40 virus–encoded small t antigen substitutes for one type of B subunit, resulting in a decrease in phosphatase activity toward MEK and an abnormal activation of the mitogenic MAPK cascade (*3*).

CK2 is a widely expressed, conserved serine-threonine kinase, the signaling function of which is obscure (*4*). Holoenzymic CK2 is a constitutively active tetramer of

catalytic (CK2α) and regulatory (CK2β) subunits; a CK2β-free pool of CK2α also exists (*5*, *6*). The region of small t antigen required for binding of PP2A (*3*) contains a sequence motif (HENRKL) that is also found between subdomains VIB and VII of the CK2α kinase domain, on what corresponds to a noncatalytic, solvent-exposed loop connecting β strands 7 and 8 in the known kinase structures (*7*) (Fig. 1A). The motif is conserved in CK2α chains from *Drosophila* to humans, but not in other kinases. The sequence was mutated as indicated in Fig. 1A, and glutathione-S-transferase (GST) fusion proteins were made with both wild-type and mutant CK2α and tested for binding to purified core PP2A in vitro. PP2A specifically bound to GST-CK2α or to the catalytically inactive mutant GST-CK2αK⁻, but not to the mutant with an altered binding domain, GST-CK2αBD (Fig. 1B). The binding-deficient mutant had the same kinase activity as wild type (*8*), ruling out a major denaturing effect of the mutation on the structure of the CK2α molecule. Although the region of CK2α required for binding to the CK2β subunit is distinct from the HENRKL motif (*9*), binding of recombinant CK2β to GST-CK2α prevented subsequent binding of PP2A (Fig. 1C). Thus, PP2A associates with free CK2α, but not with holoenzymic CK2.

In addition to binding, GST-CK2α could partially phosphorylate the PP2A dimer on the PP2Ac subunit (Fig. 1D). However, the stoichiometry of phosphorylation [up to 0.1 mol of inorganic phosphate (P_i) per mole of PP2Ac] varied among different batches of PP2A, apparently because of interference from contaminating proteins (*10*). In the presence of adenosine triphosphate (ATP), GST-CK2α, but not GST-CK2αK⁻, stimulated PP2A activity by 30 to 50%, when Raf-phosphorylated MEK1 was used as a PP2A substrate (Fig. 1E). Similar results were obtained with *p*-nitrophenylphosphate as phosphatase substrate (*10*). Therefore, CK2α-catalyzed phosphorylation appeared to enhance PP2A activity. Because PP2A rapidly dephosphorylated itself, under these conditions its activity could not be quantitatively correlated with its phosphorylation stoichiometry, and the degree of activation may be underestimated.

To determine whether CK2α binds PP2A in vivo, hemagglutinin (HA) epitope–tagged CK2α or CK2αBD was transiently expressed in NIH 3T3 cells, then immunoprecipitated with an antibody to HA (anti-HA), and an-

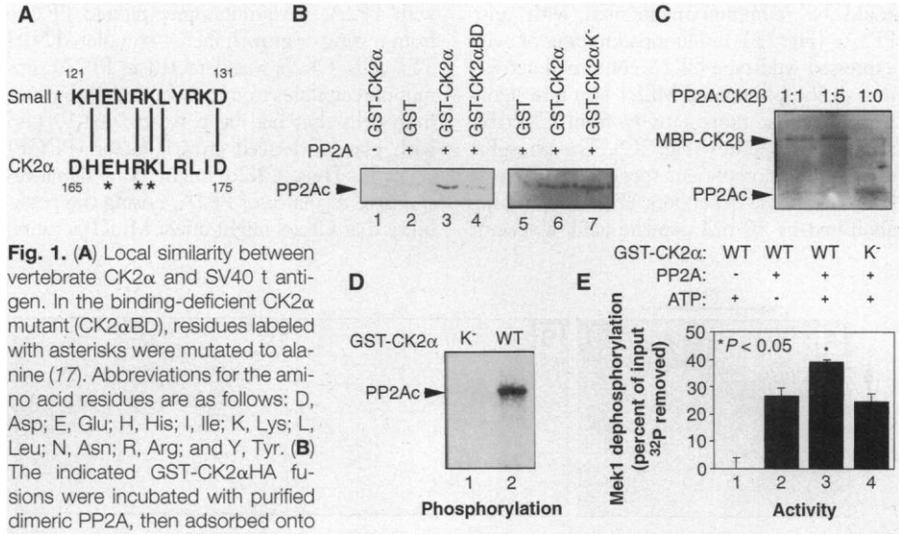

Fig. 1. (**A**) Local similarity between vertebrate CK2α and SV40 t antigen. In the binding-deficient CK2α mutant (CK2αBD), residues labeled with asterisks were mutated to alanine (*17*). Abbreviations for the amino acid residues are as follows: D, Asp; E, Glu; H, His; I, Ile; K, Lys; L, Leu; N, Asn; R, Arg; and Y, Tyr. (**B**) The indicated GST-CK2αHA fusions were incubated with purified dimeric PP2A, then adsorbed onto glutathione-Sepharose beads (*18*). After washing, the beads were analyzed by protein immunoblotting with anti-PP2Ac (*19*). (**C**) GST-CK2α was incubated with MBP-CK2β (*20*), then mixed with PP2A at the indicated MBP-CK2β:PP2A molar ratio. After adsorption to beads, the amounts of MBP-CK2β and PP2Ac bound to GST-CK2α were analyzed by immunoblotting with anti-CK2β and anti-PP2Ac. (**D**) Purified core PP2A was incubated with catalytically inactive or wild-type (WT) GST-CK2α, in the presence of [γ-^{32}P]ATP and okadaic acid (1 μM) (*15*). After boiling in 1% SDS, PP2Ac was immunoprecipitated and analyzed by SDS-PAGE and autoradiography. (**E**) The indicated mixtures were preincubated, then assayed for dephosphorylation of Raf-phosphorylated, ^{32}P-labeled His-MEK1 (*21*). Shown is the mean loss (±SD) in MEK1 phosphorylation, relative to input (n = 3) (*22*).

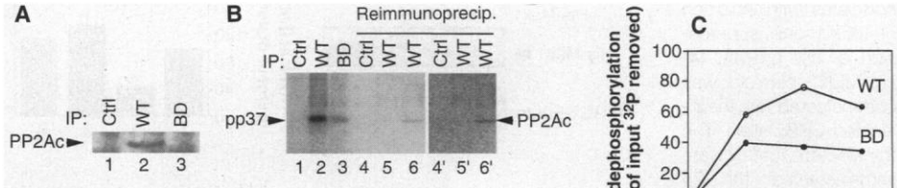

Fig. 2. Coprecipitation of endogenous PP2A with transiently expressed CK2α. (**A**) Immunoprecipitates of the indicated HA-tagged protein were analyzed by immunoblotting with anti-PP2Ac (*14*). Lane 1: Untagged CK2α. Wild-type and mutant CK2α were expressed at similar levels (*10*). (**B**) Immunoprecipitates similar to those in (A) were incubated with [γ-^{32}P]ATP (*23*), then either directly analyzed by SDS-PAGE and autoradiography (lanes 1 to 3) or eluted and reimmunoprecipitated with anti-PP2Ac (lanes 4 and 6) or control antiserum (lane 5). pp37: major autophosphorylation product. Lanes 4′ to 6′: fourfold more intense exposure of lanes 4 to 6. (**C**) Dephosphorylation of MEK1 by wild-type and binding-deficient CK2α-HA immunoprecipitates. Independent immunoprecipitates were incubated for the indicated times with ^{32}P-labeled His-MEK1 (*16*). His-MEK1 dephosphorylation was quantitated as in Fig. 1E. (**D**) The indicated numbers of cells were transfected with wild-type or control plasmids, immunoprecipitated with anti-HA, and the CK2α-HA–associated phosphatase activity was measured as the excess MEK1 dephosphorylation obtained with wild-type versus control precipitate (n = 3) (*24*). (**E**) ^{32}P-labeled His-MEK1 was incubated for 5 min with the indicated anti-HA immunoprecipitates (*16*), and MEK1 dephosphorylation was measured as above and normalized to the relative amount of immunoprecipitated CK2α-HA (n = 3). OA: 10 nM okadaic acid.

J.-K. Hériché, F. Lebrin, D. Leroy, E. M. Chambaz, Y. Goldberg, Commissariat à l'Energie Atomique, Département de Biologie Moléculaire et Structurale, Laboratoire de Biochimie des Régulations Cellulaires Endocrines, and Institut National de la Santé et de la Recherche Médicale, Unité 244, 17 avenue des Martyrs, F-38054 Grenoble Cédex 9, France.
T. Rabilloud, Commissariat à l'Energie Atomique, Département de Biologie Moléculaire et Structurale, Laboratoire de Bioénergétique Cellulaire et Pathologique, 17 avenue des Martyrs, F-38054 Grenoble Cédex 9, France.
*Present address: Institut Suisse de Recherche sur le Cancer, 155 chemin des Boveresses, CH-1066 Epalinges, Switzerland.
†To whom correspondence should be addressed.

alyzed by immunoblotting. Coprecipitating PP2A was associated with the wild-type, but not the mutant, CK2α protein (Fig. 2A). By ^{32}P labeling the CK2α immunoprecipitate in an autophosphorylation reaction, a band of similar size to PP2Ac was also detected, which could be reimmunoprecipitated with anti-PP2Ac (Fig. 2B). Immunoprecipitates of overexpressed wild-type CK2α contained activity that dephosphorylated MEK1 at a rate significantly higher than activity from CK2αBD immunoprecipitates (Fig. 2C). The phosphatase activity component specific to wild-type CK2α was dose-dependent (Fig. 2D) and was abolished by 10 nM okadaic acid, a specific inhibitor of PP2A (Fig. 2E). The MEK1 phosphatase activity associated with catalytically inactive CK2α was lower than that in wild type (Fig. 2E), possibly because CK2α kinase activates PP2A (Fig. 1E). To determine if endogenous CK2α also exists in a complex with PP2A, we immunoprecipitated PP2Ac from resting or growth factor–stimulated NIH 3T3 cells. CK2α was detected in PP2Ac immunoprecipitates from quiescent cells but not from cells that had been treated for 10 min with platelet-derived growth factor (PDGF) (Fig. 3). Thus, CK2α might be a signal-responsive regulator of PP2A, raising the possibility that CK2α might affect MEK1 activity.

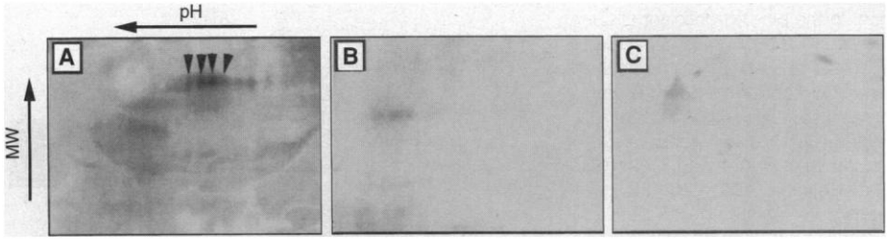

Fig. 3. Mitogen-sensitive association between endogenous CK2α and PP2A. PP2Ac was immunoprecipitated from NIH 3T3 cells that had been serum-deprived for 20 hours, then mock-treated (**A** and **B**) or stimulated with PDGF B-B (50 ng/ml) (R&D) (**C**). The immunoprecipitation in (B) was blocked with excess immunogenic peptide. The immunoprecipitates were resolved on two-dimensional gels, as described (*25*), and analyzed by protein immunoblotting with anti-CK2α (*26*). All blots were treated together with identical development of the luminescent reaction. Longer exposure of the blots showed a reduced amount of CK2α in the PDGF-treated condition (*10*). Arrows: CK2α isoforms.

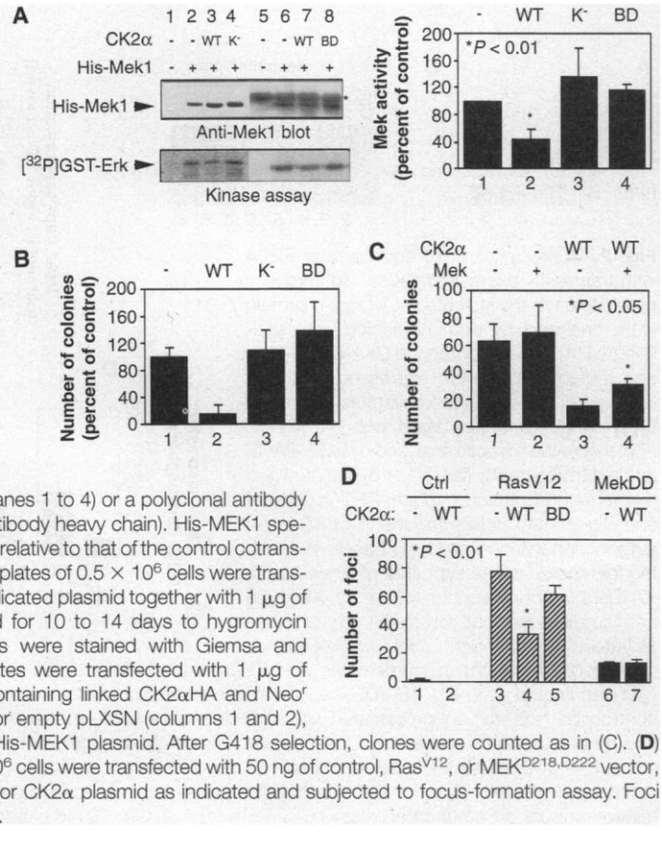

Fig. 4. Association between CK2α and PP2A correlates with inhibition of MEK1 and suppression of cell growth. (**A**) His-MEK1 plasmid was cotransfected with the indicated CK2α allele. The transfected cells were serum-starved for 24 hours, then restimulated for 10 min with fetal calf serum (20%). The His-MEK1 was purified (*27*), immunoprecipitated, assayed with catalytically inactive GST-ERK as substrate (*11*), and quantitated by immunoblotting with either a monoclonal antibody to MEK1 (lanes 1 to 4) or a polyclonal antibody (lanes 5 to 8). (Asterisk: antibody heavy chain). His-MEK1 specific activity was expressed relative to that of the control cotransfection (right). (**B**) Triplicate plates of 0.5 × 10^6 cells were transfected with 10 μg of the indicated plasmid together with 1 μg of pGK-Hygro and subjected for 10 to 14 days to hygromycin selection. Surviving clones were stained with Giemsa and counted. (**C**) Triplicate plates were transfected with 1 μg of either pLXSN-CK2αHA (containing linked CK2αHA and Neo^r genes; columns 3 and 4) or empty pLXSN (columns 1 and 2), with or without 10 μg of His-MEK1 plasmid. After G418 selection, clones were counted as in (C). (**D**) Triplicate plates of 1.5 × 10^6 cells were transfected with 50 ng of control, Ras^{V12}, or $MEK^{D218,D222}$ vector, in the presence of control or CK2α plasmid as indicated and subjected to focus-formation assay. Foci were scored after 2 weeks.

Recombinant CK2α did not inhibit MEK1 directly (*10*). However, overexpressed wild-type, but not mutant, CK2α inhibited the serum-stimulated activity of either cotransfected His-tagged MEK1 (Fig. 4A) or cotransfected HA-tagged MAPK (*10*). (The basal activity of MEK1 or MAPK was too low for evaluating its sensitivity to CK2α.) These results suggest that binding of kinase-active CK2α to PP2A may enhance PP2A activity toward MEK1 in vivo.

We selected cells that stably overexpressed CK2α. Expression of wild-type CK2α reduced cloning efficiency (Fig. 4B). This effect was partially reverted by cotransfection with wild-type MEK1 (Fig. 4C). In focus-formation assays, the outgrowth of cells transformed with Ras^{V12} [which uses activation of endogenous MEK as an effector (*11*)] was reduced by about 60% upon cotransfection of CK2α (Fig. 4D). The comparatively weak transforming activity of a constitutively activated $MEK1^{D218,222}$ mutant (*11*) was insensitive to CK2α. These results are consistent with the hypothesis that negative regulation of MEK1 is instrumental to the effect of CK2α on growth.

CK2 is required for cell proliferation (*12*). In transgenic mice, CK2α cooperates with the Myc and Scl oncogenes for the development of lymphomas (*13*). From our results, however, it appears that CK2α can negatively regulate cell proliferation. One possible explanation for this apparent paradox is that the form of CK2α that binds PP2A, and that inhibits growth, is likely free of CK2β (Fig. 1C) (6) and may thus differ from the growth-promoting form (holoenzymic CK2) (*12*). Further, because the physiological function of MEK varies with cellular context, the net proliferative effect of CK2α may also differ according to cell type.

REFERENCES AND NOTES

1. T. Hunter, *Cell* **80**, 225 (1995); D. R. Alessi *et al.*, *Curr. Biol.* **5**, 283 (1995).
2. S. Shenolikar, *Annu. Rev. Cell Biol.* **10**, 55 (1994).
3. E. Sontag *et al.*, *Cell* **75**, 887 (1993).
4. J. E. Allende and C. C. Allende, *FASEB J.* **9**, 313 (1995).
5. R. A. Heller-Harrison and M. P. Czech, *J. Biol. Chem.* **266**, 14435 (1991); J. Stigare, N. Buddelmeijer, A. Pigon, E. Egyhazi, *Mol. Cell. Biochem.* **129**, 77 (1993).
6. J.-K. Hériché *et al.*, in préparation.
7. S. K. Hanks and T. Hunter, *FASEB J.* **9**, 576 (1995).
8. Purified GST fusion proteins (2.5 ng) were incubated in triplicate reactions at 30°C for 7 min in 25 μl of kinase buffer [20 mM tris-HCl (pH 7.4), 10 mM $MgCl_2$, 14 mM β-mercaptoethanol, bovine serum albumin (BSA, 1 mg/ml)] containing 30 μM [γ-^{32}P]ATP and 10 μM CK2-specific peptide substrate (RRREDEESDDEE: R, Arg; E, Glu; D, Asp; S, Ser). Peptide phosphorylation was determined by phosphocellulose paper adsorption. Specific activities were (for GST-CK2α) 210 ± 12 and (for GST-CK2αBD) 208 ± 80 nmol P_i transferred min^{-1} mg^{-1}.
9. A. Krehan, P. Lorenz, M. Plana-Coll, W. Pyerin, *Bio-*

chemistry **35**, 4966 (1996).
10. J.-K. Hériché, F. Lebrin, Y. Goldberg, unpublished data.
11. S. Colley, H. Paterson, P. Kemp, C. J. Marshall, *Cell* **77**, 841 (1994); S. J. Mansour *et al.*, *Science* **265**, 966 (1994); G. Pagès, A. Brunet, G. L'Allemain, J. Pouysségur, *EMBO J.* **13**, 3003 (1994).
12. R. Pepperkok, P. Lorenz, R. Jakobi, W. Ansorge, W. Pyerin, *Exp. Cell Res.* **197**, 245 (1991); I. Roussou and G. Draetta, *Mol. Cell. Biol.* **14**, 576 (1994); V. Snell and P. Nurse, *EMBO J.* **13**, 2066 (1994); D. E. Hanna, A. Rethinaswamy, C. V. C. Glover, *J. Biol. Chem.* **270**, 25905 (1995).
13. D. C. Seldin and P. Leder, *Science* **267**, 894 (1995); M. A. Kelliher, D. C. Seldin, P. Leder, *EMBO J.* **15**, 5160 (1996).
14. NIH 3T3 cells (1.5×10^6) were transfected with Lipofectamine (Gibco) with 18 μg of the relevant CK2α-HA expression vector (*6*), serum-deprived for 20 hours, then lysed in 1 ml of buffer B [20 mM tris-HCl (pH 7.4), 50 mM NaCl, 50 mM NaF, 1% Triton X-100, 14 mM β-mercaptoethanol, aprotinin (25 μg/ml), leupeptin (25 μg/ml), 100 nM okadaic acid, and 0.1 mM activated vanadate]. Clarified lysates were immunoprecipitated with 1 μl of monoclonal antibody (12CA5) to HA and 25 μl of protein A–Sepharose. Immunoprecipitates were washed three times in buffer B and once in tris-buffered saline [20 mM tris-HCl (pH 7.4), 150 mM NaCl] containing 100 nM okadaic acid and subjected to chemiluminescent immunoblotting.
15. PP2A (500 ng) was incubated at 30°C for 20 min with 5 ng of GST-CK2α in 30 μl of kinase buffer containing 100 μM [γ-^{32}P]ATP (10^4 dpm/pmol) and okadaic acid (1 μM). Then, 30 μl of 2% SDS was added, the mixture was heated at 100°C for 5 min, diluted into 540 μl of 20 mM tris-HCl (pH 7.4), 150 mM NaCl, 1% Triton X-100, 0.5% sodium deoxycholate, and BSA (1 mg/ml), and immunoprecipitated with 2 μl of anti-PP2Ac.
16. Immunoprecipitates (*14*) were prepared without okadaic acid and incubated with 60 ng of the Raf1-phosphorylated MEK1 at 20°C in 30 μl of kinase buffer without $MgCl_2$. Reactions were analyzed by SDS–polyacrylamide gel electrophoresis (PAGE) and autoradiography.
17. C. S. Gibbs and M. J. Zoller, *J. Biol. Chem.* **266**, 8923 (1991); I. Mikaelian and A. Sergeant, *Nucleic Acids Res.* **20**, 376 (1992).
18. Wild-type and mutant chicken CK2α cDNAs were subcloned (as HA-tagged derivatives) in frame with GST and expressed in *Escherichia coli* BL21(DE3). GST fusions were purified by glutathione-Sepharose chromatography as recommended by the manufacturer (Pharmacia). The purified GST fusions (200 ng) were incubated with purified PP2A dimer (200 ng, UBI) in 100 μl of kinase buffer for 20 min at 25°C. The mixture was adsorbed to glutathione-Sepharose in buffer A [20 mM tris-HCl (pH 7.4), 50 mM NaCl, 0.1% Triton X-100, 14 mM β-mercaptoethanol] for 30 min at 4°C. The beads were washed three times in buffer A, eluted into Laemmli buffer, and analyzed by chemiluminescent immunoblotting.
19. E. T. Ulug, A. J. Cartwright, S. A. Courtneidge, *J. Virol.* **66**, 1458 (1992).
20. CK2β was subcloned into the pMAL vector (New England Biolabs), expressed as a maltose-binding protein (MBP)–CK2β fusion, and purified by chromatography on amylose beads.
21. PP2A dimer (10 ng, 20 mU) was incubated for 15 min at 30°C with GST-CK2α (2 ng), with or without 100 μM ATP. Bacterially produced His-MEK1 (100 ng) that had been ^{32}P-labeled in vitro by immunoprecipitated Raf [J. R. Fabian, A. B. Vojtek, J. A. Cooper, D. K. Morrison, *Proc. Natl. Acad. Sci. U.S.A.* **91**, 5982 (1994)] and repurified was added and incubated for a further 15 min. Reactions were directly analyzed by SDS-PAGE and PhosphorImager quantitation of the His-MEK1 bands.
22. All probabilities were computed by Student's *t* test with Scheffe's correction for multiple comparisons.
23. Immunoprecipitates were incubated for 15 min at 25°C in 30 μl of kinase buffer containing 20 μM [γ-^{32}P]ATP (10^4 dpm/pmol). Reactions were stopped by adding Laemmli gel buffer and heating at 100°C. For reimmunoprecipitation (*15*), 10 μM [γ-^{32}P]ATP (10^5 dpm/pmol) was used.
24. Cells were transfected with Lipofectamine with 6 μg of plasmid per 0.5×10^6 cells. All lysates were immunoprecipitated with 1 μl of 12CA5 and assayed for 10 min as above (*16*).
25. T. Rabilloud, C. Valette, J. J. Lawrence, *Electrophoresis* **15**, 1552 (1994).
26. O. Filhol, C. Cochet, E. M. Chambaz, *Biochemistry* **29**, 9928 (1990).
27. Cells (1.5×10^6) were transfected by calcium phosphate precipitation with a mixture of 2 μg of CK2α, 8 μg of His-MEK1, and 12 μg of carrier plasmid. Cells were lysed in buffer B containing 100 mM NaCl (*14*), and His-MEK1 was adsorbed onto 20 μl of nickel-trinitriloacetate resin (Invitrogen) for 1 hour at 4°C, washed three times in lysis buffer, and eluted into 50 μl of lysis buffer containing BSA (1 mg/ml) and 0.25 M imidazole (pH 7.4).
28. We thank S. A. Courtneidge for anti-PP2A and peptide; A. Brunet and J. Pouysségur for the HA-MAPK and MEKD constructs; U. R. Rapp for anti-Raf; J. Ghysdael for the Raf1 baculovirus; T. Sturgill for the SrcF527 and v-Ha-Ras baculoviruses; A. Berns and C. Ovitt for the pGKHygro plasmid; and J. Ghysdael, D. Job, and our laboratory colleagues for critically reviewing the manuscript. J.-K.H. was supported by the Ministère de l'Enseignement Supérieur et de la Recherche and by the Ligue Nationale contre le Cancer. Supported by Commissariat à l'Energie Atomique, INSERM, and CNRS.

25 June 1996; accepted 5 March 1997

Structures of the Tyrosine Kinase Domain of Fibroblast Growth Factor Receptor in Complex with Inhibitors

Moosa Mohammadi, Gerald McMahon, Li Sun, Cho Tang, Peter Hirth, Brian K. Yeh, Stevan R. Hubbard,* Joseph Schlessinger*

A new class of protein tyrosine kinase inhibitors was identified that is based on an oxindole core (indolinones). Two compounds from this class inhibited the kinase activity of fibroblast growth factor receptor 1 (FGFR1) and showed differential specificity toward other receptor tyrosine kinases. Crystal structures of the tyrosine kinase domain of FGFR1 in complex with the two compounds were determined. The oxindole occupies the site in which the adenine of adenosine triphosphate binds, whereas the moieties that extend from the oxindole contact residues in the hinge region between the two kinase lobes. The more specific inhibitor of FGFR1 induces a conformational change in the nucleotide-binding loop. This structural information will facilitate the design of new inhibitors for use in the treatment of cancer and other diseases in which cell signaling by tyrosine kinases plays a crucial role in disease pathogenesis.

Protein tyrosine kinases (PTKs) are critical components of signaling pathways that control cell proliferation and differentiation. Enhanced PTK activity due to activating mutations or overexpression has been implicated in many human cancers (*1*). Thus, selective inhibitors of PTKs have considerable therapeutic value (*2*). Although a number of compounds have been identified as effective inhibitors of specific PTKs, the precise molecular mechanisms by which these agents inhibit PTK activity have not been elucidated.

Fibroblast growth factors (FGFs) play important roles in embryonic development, angiogenesis, wound healing, and malignant transformation (*3*). The diverse effects of mammalian FGFs are mediated by four transmembrane receptors (FGFR1 through FGFR4) with intrinsic PTK activity (*4*). Activating mutations in FGF receptor genes have been implicated in various human skeletal disorders such as Crouzon syndrome (*5*), achondroplasia (*6*, *7*), and thanatophoric dysplasia (*7*, *8*). Inappropriate expression of FGFs or activation of FGF receptors could contribute to several human angiogenic pathologies such as diabetic retinopathy, rheumatoid arthritis, atherosclerosis, and tumor neovascularization (*9*). Moreover, genes encoding FGFR1 and FGFR2 were shown to be amplified in a population of breast cancers (*10*). verexpression of FGF receptors has also been detected in human pancreatic cancers (*11*), astrocytomas (*12*), salivary gland adenosarcomas (*13*), Kaposi's sarcomas (*14*), ovarian cancers (*15*), and prostate cancers (*16*).

We identified a new family of inhibitors for receptor tyrosine kinases by screening a library of synthetic compounds. A new class of PTK inhibitors was generated by attaching different chemical substituents to an oxindole core (indolinones). These com-

M. Mohammadi, B. K. Yeh, J. Schlessinger, Department of Pharmacology, New York University Medical Center, New York, NY 10016, USA.
G. McMahon, L. Sun, C. Tang, P. Hirth, SUGEN, Redwood City, CA 94063, USA.
S. R. Hubbard, Skirball Institute of Biomolecular Medicine and Department of Pharmacology, New York University Medical Center, New York, NY 10016, USA.
*To whom correspondence should be addressed.